RESEARCH

Influence of prosthetic index structures and implant materials on stress distribution in implant restorations: a three-dimensional finite element analysis

Annikaer Anniwaer[1†], Aihemaiti Muhetaer[1†], Zhengrong Yin[1], Jiakang Zhu[1], Chunxiao Jin[1] and Cui Huang[1*]

Abstract

Background Mechanical complications affect the stability of implant restorations and are a key concern for clinicians, especially with the frequent introduction of new implant designs featuring various structures and materials. This study evaluated the effect of different prosthetic index structure types and implant materials on the stress distribution of implant restorations using both in silico and in vitro methods.

Methods Four finite element analysis (FEA) models of implant restorations were created, incorporating two prosthetic index structures (cross-fit (CF) and torc-fit (TF)) and two implant materials (titanium and titanium-zirconium). A static load was applied to each group. An in vitro study using digital image correlation (DIC) with a research scenario identical to that of the FEA was conducted for validation. The primary strain, sensitivity index, and equivalent von Mises stress were used to evaluate the outcomes.

Results Changing the implant material from titanium to titanium-zirconium did not significantly affect the stress distribution or maximum stress value of other components, except for the implant itself. In the CF group, implants with a lower elastic modulus increased the stress on the screw. The TF group showed better stress distribution on the abutment and a lower stress value on the screw. The TF group demonstrated similar sensitivity for all components. DIC analysis revealed significant differences between TF-TiZr and CF-Ti in terms of the maximum ($P < 0.001$) and minimum principal strains ($P < 0.05$) on the implants and the minimum principal strains on the investment materials in both groups ($P < 0.001$).

Conclusions Changes in the implant material significantly affected the maximum stress of the implant. The TF group exhibited better structural integrity and reliability.

Keywords Implant, Screw, Stress distribution, Digital image correlation test

†Annikaer Anniwaer and Aihemaiti Muhetaer contributed equally to this work and should be regarded as co-first authors.

*Correspondence:
Cui Huang
huangcui@whu.edu.cn

[1]State Key Laboratory of Oral & Maxillofacial Reconstruction and Regeneration, Key Laboratory of Oral Biomedicine Ministry of Education, Hubei Key Laboratory of Stomatology, School & Hospital of Stomatology, Wuhan University, #237 Luoyu Road, Hongshan District, Wuhan 430079, China

Introduction

Fifty years ago, the discovery that titanium implants can achieve anchorage in bone tissue through direct bone-to-implant contact revolutionized the restoration of missing teeth with dental implants [1]. The structural design of these implants continues to evolve to address critical clinical situations, with modifications including both external and internal alterations.

The mechanical design parameters associated with external modifications of the implant body primarily concern the thread type, pitch, depth, and width. Changes in these parameters result in different performance outcomes for implant restorations. Four finite element analyses (FEA) revealed that implants with smaller thread sizes and shorter pitch lengths caused greater bone stress [2]. Another study comparing the effects of different thread profiles on stress distribution in peri-implant bone revealed that compared with other thread types, square threads produced more favorable stress on peri-implant hard tissue [3]. Additionally, microthreads in the neck portion of the implant increase stress concentrations in cortical bone [4].

Internal structural changes have a significant biomechanical influence on implant restorations. According to the treatment guidance of the International Team for Implantology (ITI), at least eight interfaces exist within implant restorations and are significantly influenced by changes in connection type [5]. These modifications notably affect force transmission within the internal structure. Implants with an external connection exhibit more stress in the screws under oblique loading than do those with an internal connection [6]. Furthermore, a greater internal connection angle led to less screw loosening due to loading, indicating improved preload maintenance [7]. According to a retrospective study, abutment fractures occurred more frequently within single crowns according to the positioning index [8]. Therefore, each structural change significantly influences the stress-related performance of different implant designs.

Stress, defined as the pressure exerted on the cross-sectional area of a substance, is closely connected to deformation or fracture and is the main cause of mechanical complications in the clinic. This value is strongly affected by the chemical composition and microscopic structure of the material. Therefore, stress-related performance differences in implant systems are crucial for preventing serious complications. Titanium-related materials are considered ideal for dental implants [9]. With the improvement of titanium-related binary alloys [10], a wider range of materials with varying biomechanical performances are now available [11]. The advancement of materials science has also introduced nonmetallic materials for implant and abutment selection [12]. However, these innovative nonmetallic materials still carry a risk of abrasion in the connecting part and fracture under functional loads [13, 14]. Metallic materials remain the primary choice in most clinical scenarios. While implant materials often undergo modifications to enhance their mechanical properties, such alterations are less frequent in abutment materials. The potential effect of these material differences on the biomechanical properties of the entire implant system is still being investigated. Additionally, it is worthwhile to examine the stress-related sensitivity of each component under both material and structural factors.

Therefore, this stress analysis aimed to assess the biomechanical effect of implant material and connection type on implant restorations in silico and in vitro. The experimental hypotheses were that differences in implant material would present significant differences in the biomechanical capacities of all components in the implant system, and each test result would vary across different structure groups.

Methods

In silico analysis method

Finite element modeling

3D models of implant restoration were created using computer-aided design software based on micro-CT images and product descriptions. Images of the implant-related metal structures were obtained using micro-CT (Sky Scan 1276, Germany) and reconstructed and measured using reconstruction software (NRecon 1.7.4.6, Germany; Mimics Research 21.0, Belgium). Modeling software (SolidWorks, USA) was used to produce more precise 3D models.

For both groups, a simplified crown made of cobalt-chromium alloy (Co-Cr) was reconstructed according to the International Organization for Standardization (ISO)-14801:2016 standards. These models were distributed in their respective study groups: the cross-fit (CF) group, consisting of a titanium implant (4.8×12 mm; BL, Straumann) and titanium abutment (RC Variobase, Straumann); and the torc-fit (TF) group, comprising a titanium implant (4.5×12 mm; BLX, Straumann) and titanium abutment (RB Variobase, Straumann). The CF group was considered the control group. Furthermore, the two aforementioned groups were divided into four subgroups based on alterations in implant materials from titanium alloy to titanium-zirconium alloy: CF-Ti, CF-TiZr, TF-Ti, and TF-TiZr. Micro-CT images of the actual implant restorations validated the assembly of each 3D component in the two groups (Fig. 1). All assembled models were solidified in cylindrical investment material (H: 18 mm; D: 30 mm) that could be attached to a platform with a 30-degree incline.
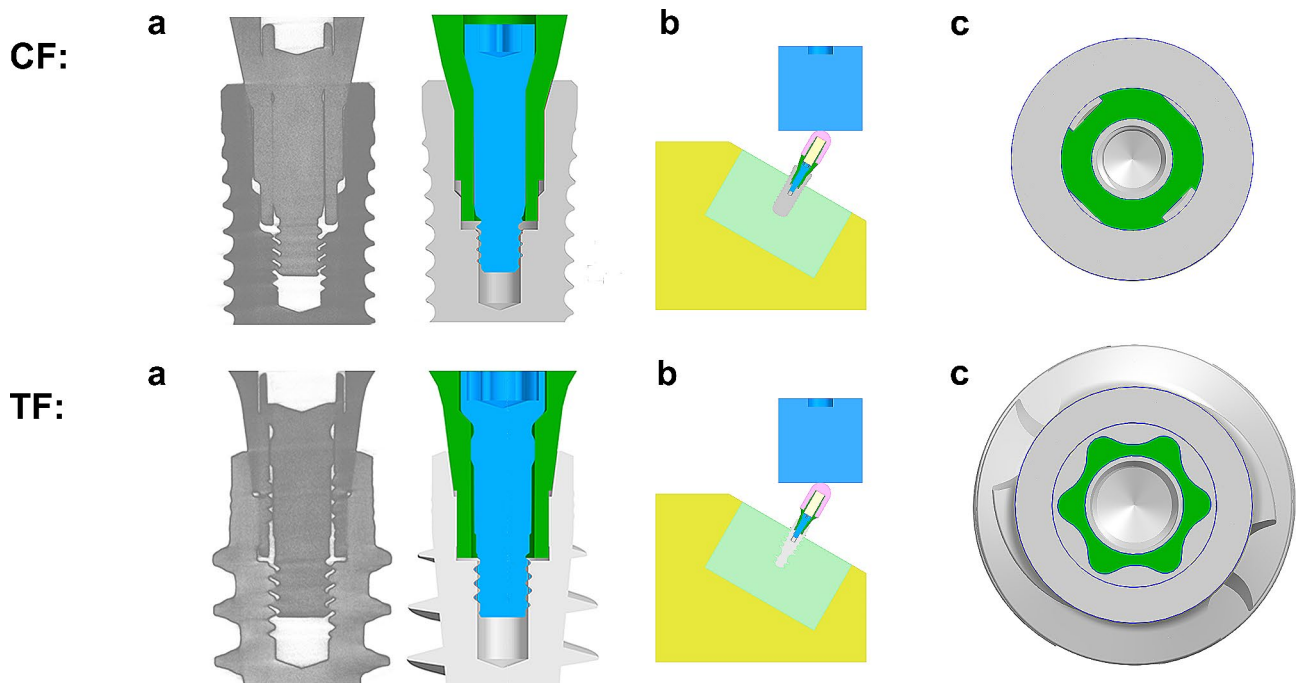
Anniwaer *et al. BMC Oral Health*   (2024) 24:901

Page 3 of 11

Fig. 1 Assembly of each 3D component in the two groups. (**a**: Validation of the assembling relation; **b**: final assembled model; **c**: top view of the prosthetic index structures)

Table 1 Materials properties

Structure	Materials	Young's modulus (GPa)	Poisson's ratio	Data from
CF Implant	Ti-Grade4	110	0.33	[16]
TF Implant	Ti-Grade4	110	0.33	[16]
CF Implant	Ti-Zr	96.12	0.3	[17, 18]
TF Implant	Ti-Zr	96.12	0.3	[17, 18]
Abutment/Screw	TAN(TiAlNb)	110	0.37	[19, 20]
Crown	Co-Cr	220	0.30	[21]
Investment Materials (Base)	PMMA	8.3	0.28	[22]
Resin	Z100	18	0.24	[23]

Finite element analysis

The 3D models were imported into computer-aided engineering software (ANSYS Workbench ver. 13.0, USA) for finite element analysis. The materials were assumed to be isotropic, homogeneous, and linearly elastic. The contacts were considered to have intimate contact (no friction) except for the implant/abutment, abutment/screw, and screw/implant interfaces, where a coefficient of friction of 0.30 was applied for the titanium-titanium [15]. The values for Young's modulus and Poisson's ratio are described in Table 1 [16–23]. The screw torque followed the manufacturer's guidelines of 35 N/cm for each group. To define the screw torque, a body force was applied to the middle part of the abutment screw shank where screw elongation was expected with tightening.

A load of 130 N at a 30-degree angle relative to the implant axis at the top portion of the crowns was applied in each group [24]. During mesh generation, the SOLID187 element type was selected. The element sizes were customized to 2.0 mm for the investment material, 0.5 mm for the implant-associated components, and 0.1 mm for the threads. To ensure a mesh-size-independent and stable solution, particularly in the impact zone, a refinement process was implemented to ensure the utmost precision in this critical area. Additionally, the mesh quality was rigorously evaluated using metrics such as the Jacobian ratio, aspect ratio, maximum corner angle, and skewness. Finally, a convergence test was performed, in which the mesh density was progressively increased until the maximum stress in the implant exhibited a variation of less than 5%, thus ensuring the reliability of the results. A supercomputer (32C96G, Intel(R) Xeon(R) Gold 6130 CPU @ 2.10 GHz) was utilized to increase the computational speed and accuracy. The models with triangular surfaces presented various numbers of elements and nodes, as depicted in Table 2.

In vitro mechanical test

Model fabrication and experimental setting

A priori power analysis using G*Power software [25] was conducted based on the results of the pilot study and previous research, with an effect size of 2.5, a power of 95%, and an α of 0.05. It was determined that 5 specimens per group would be sufficient. Ten commercial

Anniwaer *et al. BMC Oral Health*   (2024) 24:901

Page 4 of 11

Table 2 The final results of the 3D FE models

Materials		Node	Element
Crown	CF	11,846	7421
	TF	11,809	7487
Abutment	CF	8931	4884
	TF	28,924	16,245
Screw	CF	15,697	8956
	TF	17,582	9981
Implant	CF	217,661	128,388
	TF	252,952	145,826
Investment Materials (Base)	CF	203,169	123,641
	TF	247,521	152,084
Resin	CF	2234	435
	TF	1689	325

implants, representing the CF-Ti group and the TF-TiZr group, were embedded in the center of a cylindrical silicone mold filled with polymethyl methacrylate material (Truer, China). This procedure was performed under the guidance of a 3 mm thick CAD/CAM guide plate, which ensured a consistent correct position, axial alignment, and a 3 mm distance between the implant shoulder and the first implant-resin contact, in accordance with ISO-14801:2016. All specimens were solidified in a polymethyl methacrylate cylinder base (H: 18 mm; D: 30 mm) and could be fixed on the center of a specially made loading platform with a 30° slope. For these samples, the matching abutment and crown were assembled, and all screws were tightened to 35 N/cm.

In this in vitro mechanical test, a digital image correlation measurement system (VIC-2D; Correlated Solutions) was used to measure the full-field displacements and surface strains of the material samples. Speckle patterns were randomly placed on the surface of the specimens, which had already been painted white by spraying the black coating material in free-fall from the same distance. Then, an in vitro mechanical test was conducted for the three implant systems in this study. The crown was gradually loaded with an axial 130 N load on its top portion over a period of 0.5 s using a universal testing machine (E1000, INSTRON, USA).

Digital Image Correlation (DIC) measurements

An experimental framework utilizing a digital image correlation (DIC) system was employed to quantify the full-field deformation and surface strain of each implant system. The system consisted of a camera equipped with charge-coupled devices (FASTCAM SA5, Photron, Japan) and Nikon lenses, set at a resolution of 1024×1024 pixels. The camera had a measurement frequency of 500 frames/second. To enhance the visibility and contrast of the surface speckle pattern, a light-emitting diode lamp with polarized filters was used (Fig. 2). The region of interest for DIC and strain measurement was set at a size of 50×30 pixels at the abutment, implant wall, and investment material for all specimens. The linear strain algorithm in VIC 2D software (Correlated Solutions, USA) was utilized to calculate the average strains based on the displacements at the data points. The recorded strains included the maximum (e1) and minimum (e2) principal strains, which were analyzed for each test. The normality of the independent samples was assessed using the Shapiro−Wilk test to ensure the validity of subsequent parametric analyses. After confirming normality, an independent samples t test was conducted to compare the mean values between the groups. All the statistical analyses were performed using SPSS Statistics version 23 (IBM, USA), with a significance level set at $P<0.05$ to determine the statistical significance and ensure rigorous evaluation of the results.
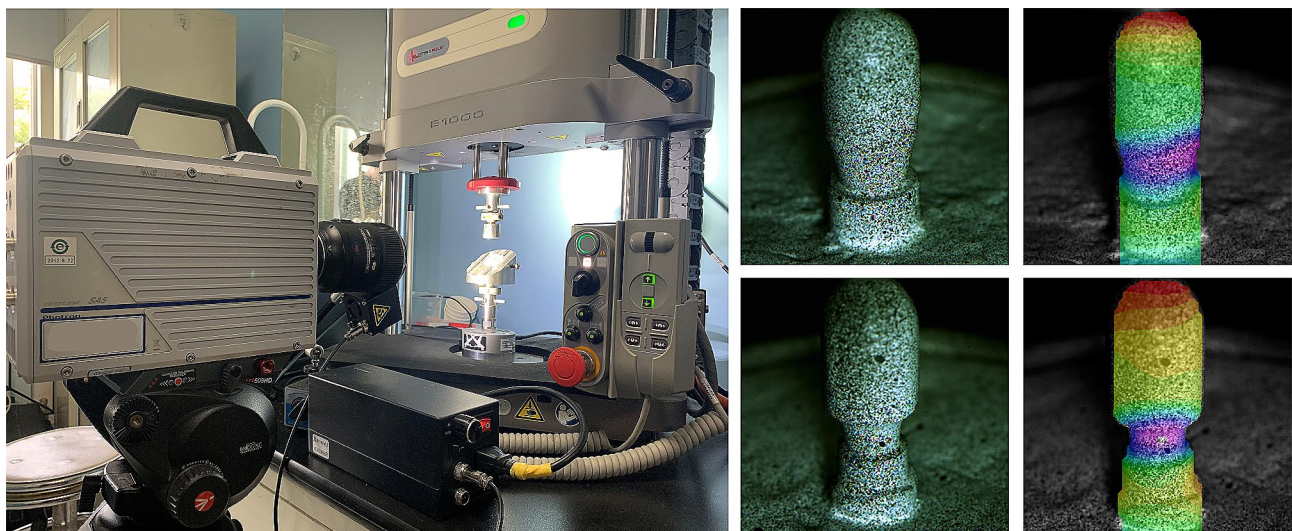
Fig. 2 DIC process for each group

Results

Overall stress distribution

The FEA results showed that when the screws were tightened and static loads were applied, stress was distributed throughout the entire screw body in each system. There was less stress on the screw head but more stress on the screw thread. The abutment and investment material exhibited the lowest maximum stress values. The TF group demonstrated a more favorable stress distribution on the abutment but had greater stress on the overall implant body. The change in implant alloy type did not significantly affect the stress distribution in each component (Fig. 3).

The principal strain and maximum Von Mises stress of the implant systems

For in vitro evaluation, the principal strains of the two groups were tested using digital image correlation methods. The maximum principal strains were tensile, whereas the minimum principal strains were compressive around the transmucosal part of the abutment, cervix of the implant, and investment material. Structural design differences may not have a noticeable influence on the two types of principal strain in the abutment of the two implant systems ($P > 0.05$). However, significant differences were observed in the maximum ($P < 0.001$) and minimum principal strains on the implant ($P < 0.05$), as well as in the minimum principal strains on the investment materials between the two groups ($P < 0.001$) (Fig. 4).
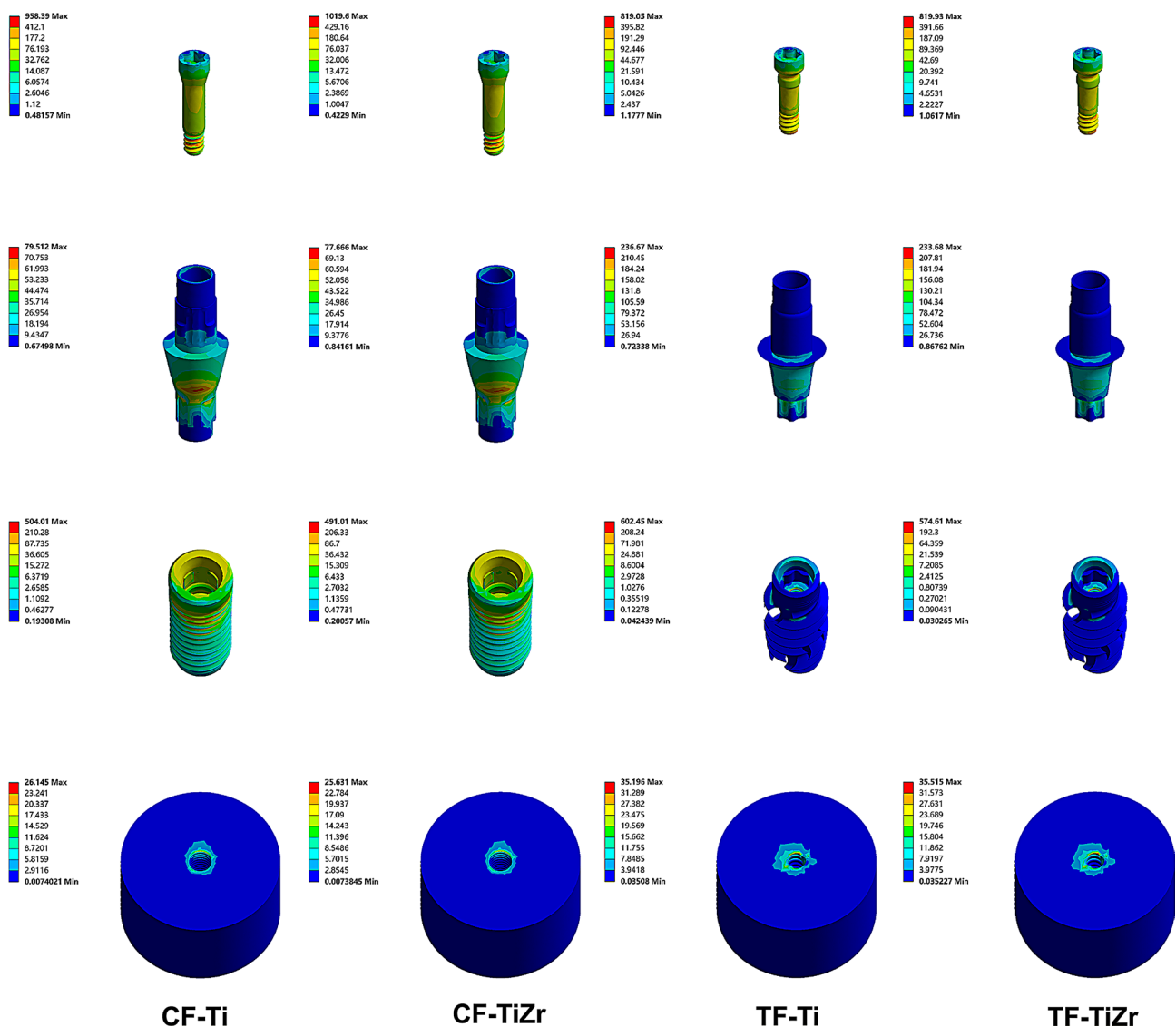

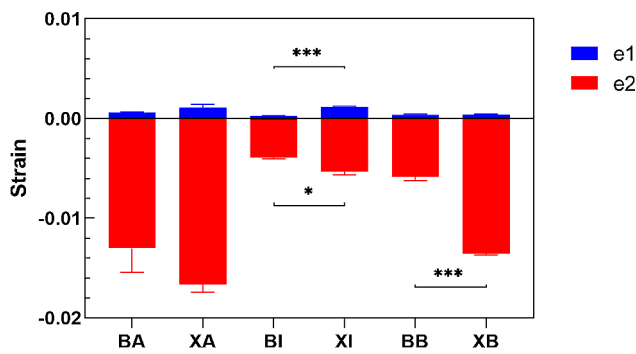**Fig. 3** Equivalent stress distribution of each component in the two systems

Fig. 4 Strain data: e1 represents the maximum and e2 represents the minimum principal strains. (A: abutment; I: implant; B: base; **: $P < 0.01$, ***: $P < 0.001$)
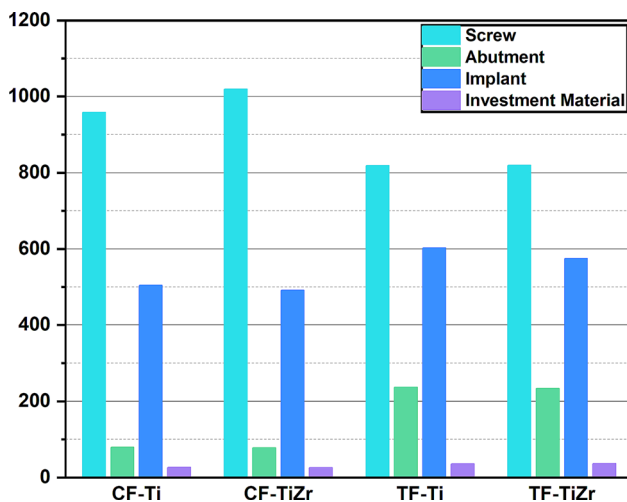

Fig. 5 Maximum von Mises equivalent stress of each component in the three groups (MPa).

According to the FEA results, the stress pattern differed between the two implant systems. The differences in the maximum stress were primarily concentrated on the abutment, screw, and implant. In the CF-TiZr group, the maximum stress was greater than that in the other groups, reaching 1019 MPa. On the other hand, the TF-Ti group exhibited the highest maximum stress, with the stress of the implants reaching 602 MPa and that of the abutments reaching 237 MPa. The change in implant alloy type did not have a significant impact on the maximum stress in the abutment or the investment materials, but it did have a greater effect on the maximum stress in the implant itself. Additionally, when the implant material was changed from titanium to titanium-zirconium, the maximum stress of the screw in the CF group increased significantly from 958 MPa to 1019 MPa (Fig. 5).

Sensitivity analysis

To investigate how the variation in implant materials or structure affects the stress distribution in each structure of implant restorations under loads, a sensitivity analysis based on the von Mises maximum and minimum stress values from the FEA results was conducted [26].

$$\text{Sensitivity (\%)} = (\text{Max. stress} - \text{Min. stress})/\text{Max. stress} \times 100\%$$

A summary of the analyses is presented in Fig. 6. The sensitivity analysis revealed that the sensitivity to connection alterations exceeded that of implant material alterations for each component. Specifically, these factors had the least influence on the abutments, especially in the CF group. However, the TF group demonstrated similar sensitivity in the screw, abutment, implant, and bone, which indicates that they may have better stress distribution as a whole rigid part.

DIC validation

The surface strains and full-field deformation of both implant systems were measured experimentally using the DIC system. It is noteworthy that the deformation contours obtained through the DIC technique aligned with the numerical outcomes for all the prostheses, and the strain trend was consistent with the stress results of the FEA, indicating the accuracy and efficiency of the model construction (Fig. 7). However, the experimental strains exhibited some concentrations in the form of artifacts at the abutment and implant regions. Achieving a perfect match between the DIC strain contour distribution and magnitude with those of FEA can be challenging due to the small strain measurements involved [27]. The complex structure of the implant-supported prosthesis model, the small size of the regions of interest, and the obstruction of surface speckle patterns could be contributing factors to this issue.

Discussion

In this study, two 3D models of implant restorations were created using micro-CT images and product profiles, which differed in terms of their connection type. Two distinct Young's moduli were incorporated into the implant, resulting in the formation of four subgroups. We then analyzed the influence of material and structure on the stress and distribution of each component in the implant restorations. The materials used and loading conditions followed strict adherence to ISO standards and relevant previous research, ensuring the acceptability of the study's results for analysis and comparison.

To enhance the reliability of the FEA results, digital image correlation methods were employed to observe the strain conditions of two existing commercial implant systems (CF-Ti and TF-TiZr) under identical experimental conditions. Our findings revealed that the stress values and distribution of each component change when
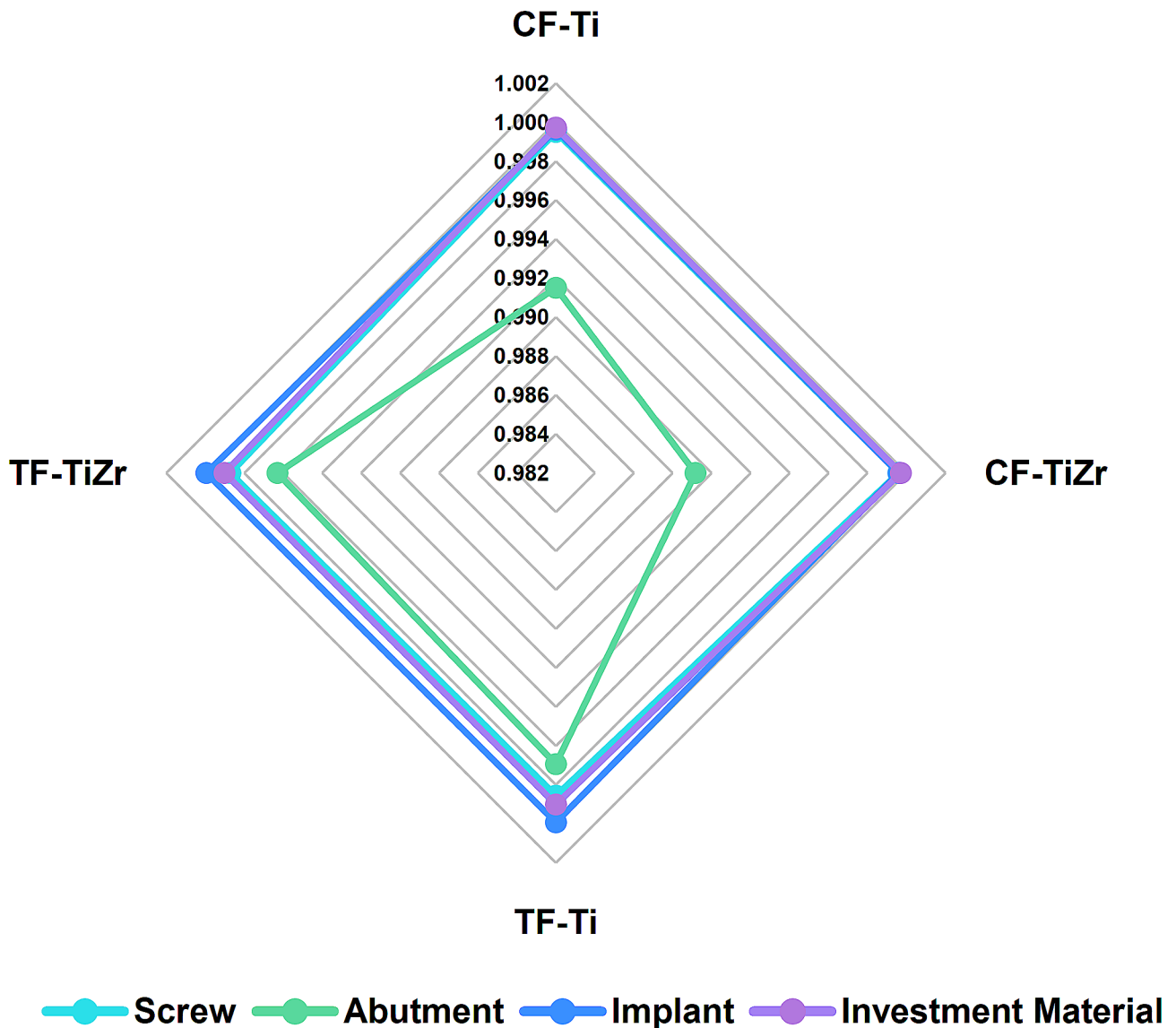
Fig. 6 Sensitivity analysis results for each group

transitioning from CF to TF structures. Among the affected components, the screw is the most influenced, followed by the abutment and implant. Furthermore, compared with changes in the other components, material changes in the implant had a greater impact on the maximum stress of the implant itself in the TF group. However, such material changes significantly affected both the maximum stress of the screw and implant in the CF group, both in vitro and in silico. Additionally, the TF group demonstrated similar sensitivities to the screw, abutment, implant, and investment material, suggesting better stress distribution as a whole rigid part. Therefore, our study refutes the first experimental hypothesis and proposes the second as an alternative explanation.

The mechanical characteristics of materials are determined by several factors at the chemical and microstructure levels, including changes in bond energy, atom size, types of chemical bonds, crystal size, number of crystal borders, and dislocation density. Consequently, the material type has a profound influence on the mechanical properties of each material. In this study, implant-related components made from the same material were assembled with two different types of implants, namely, titanium and titanium-zirconium. The FEA results indicated that changing the material in the implant primarily affected the stress value within the implant itself, with no significant stress changes observed in the other related components. This conclusion is further supported by the DIC results. Previous investigations have revealed that the mechanical properties of implant restorations are affected by material differences between their components. For instance, a systematic
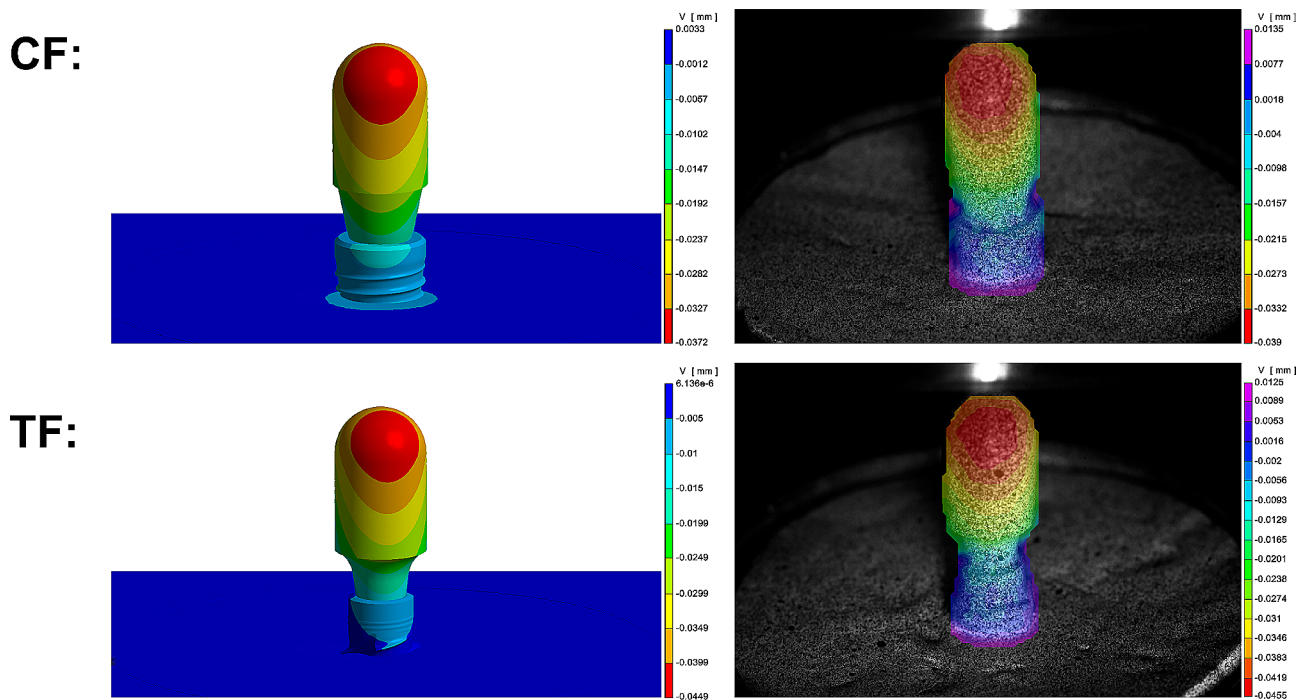
Fig. 7 Correlation between the FEA and DIC results

analysis of 90 studies demonstrated that zirconia abutments produce more wear at the interface between the abutment and the titanium implant [28]. This finding is consistent with an earlier study suggesting that differences in material hardness can lead to varying levels of wear [29]. Furthermore, zirconia abutments tend to concentrate more stress throughout the prosthetic system and may be more prone to mechanical problems than titanium abutments [30]. Another stress analysis revealed that titanium implants result in a more uniform stress distribution than zirconium implants [31]. Interestingly, in this study, the influence of material on the outcomes was not particularly conspicuous, which is consistent with a previous FEA investigation that compared the stress distribution differences between tissue-level and bone-level implant body designs using commercial titanium and titanium-zirconium implants [32]. This similarity can be attributed to the relatively similar values of Young's modulus and tensile strength between the two materials. Specifically, the Young's moduli of titanium and titanium-zirconium are approximately 110 GPa and 96.12 GPa, respectively, and the tensile strengths of titanium and titanium-zirconium are approximately 851 MPa and 968 MPa, respectively. Therefore, in the current scenario, a change in the metallic material used for assembly may not significantly affect the force transfer as long as the assembly relations are correct. However, it is worth mentioning that this study did not involve in vitro testing of different implant materials with the same structure, as such commercial product types are not yet available. Therefore, further confirmation of this conclusion through in vitro testing is still necessary.

The implant-abutment interface (IAI) is a critical connection between the implant and abutment and plays a crucial role in the biological stability of the implant by ensuring microgap sealing. This sealing is essential for joint strength and stability [33]. In internal connection implant systems, the IAI consists of connection and prosthetic index parts. The connection parts can be categorized as external or internal, depending on whether the mating components are recessed into the implant body. Additionally, these connection parts can be classified as conical or nonconical based on the presence or absence of a tapered design. The tapered design has different effects on implant restorations. A systematic review was conducted to compare the performance of internal tapered and internal nontapered connections, and the results showed that the tapered connection exhibited significantly reduced marginal bone loss and probing depths compared to the nontapered connection [34]. Another study also confirmed that the tapered connection may be a more favorable treatment option, as it preserves more peri-implant bone and reduces the risk of prosthodontic complications [35]. Another important component of the IAI is the prosthetic index, which is a special structure designed to resist rotation or twisting forces. These parts are commonly used on the abutment bottom surfaces to stabilize the upper structure, thereby making each component of the implant restorations a rigid whole. In an in vitro study, it was found that engaging abutments

are 17 times more stable than prostheses supported by nonengaging abutments [36]. Furthermore, different types of engagement systems have varying effects on the mechanical properties of structures. Previous studies have shown that abutment connections with CFs significantly decrease lateral movement [37], and a new connection called the octatorx has a smaller microgap and greater torque resistance than the traditional internal hexagon connection [38]. In this study, two commercial conical implant systems with different prosthetic indices were utilized: a conical connection with the CF index and a conical connection with the TF index. This difference results in varying stress values in each component, even though the Young's modulus of the implant in the CF and TF groups was altered to that of titanium and titanium-zirconium. The maximum stress value was found in the CF groups. The TF design provides an enlarged contact surface, increasing the friction-based retention force for the abutment and reducing the reliance on screws for retention. This leads to a transfer of stress from the screws to other components in the TF groups, resulting in decreased stress on the screws. The FEA results indicate a larger stress distribution area and greater stress on the TF abutment neck, supporting the aforementioned hypothesis. Conversely, the CF group exhibited relatively greater stress on the screw. The differences in abutment sensitivity among the four groups also support this conclusion. An in vitro study evaluating the removal torque for TF and CF revealed that the CF groups exhibited greater removal torque than did the TF group, which may suggest that the screws in the CF groups were under greater stress [39]. Therefore, structural design remains the primary factor affecting the mechanical properties of implant restorations. However, further multiscale evaluations focusing on the micromovement and integrity of this connection type in vitro are still needed.

Although FEA is commonly used in solid mechanics to solve partial differential equations, it is still necessary to validate FEA to ensure that the simulation results accurately reflect real-world results. Digital photoelasticity takes advantage of the fact that birefringent bodies can provide stress information through color fringe patterns [40]. On the other hand, DIC is a full-field strain gauging method that captures the speckle on an object and measures displacement [41, 42]. Some studies validate FEA results by comparing the scanning electron microscopy (SEM) image of the crack structure after fatigue testing with the stress concentration results obtained through FEA [43]. In addition, retrospective clinical data on stress-related complications are also used to validate FEA results in certain research studies [44]. In this particular study, the authenticity of the mimics was improved by using micro-CT images and product descriptions, but DIC methods were still employed to confirm the stress

analysis results. It is worth noting that the deformation contours obtained through DIC agreed with the FEA results in the contrasting groups. However, even though the conditions of the in vitro experiment were consistent with those of the FEA, a higher level of consistency in the deformation results between the two studies was not achieved at the numerical level. This could be attributed to the complexity of the implant-supported prosthesis model, the limited size of regions of interest, and the obstruction of surface speckle patterns. Therefore, additional multiscale evaluation techniques are still required to validate the FEA results. Furthermore, the Shapiro–Wilk test is commonly used to assess the normality of a sample. However, it is important to acknowledge that this test has certain assumptions and limitations. One of the main assumptions of the Shapiro–Wilk test is that the data are independently and identically distributed. Violations of this assumption can lead to inaccurate results. Additionally, the Shapiro–Wilk test may be sensitive to outliers and small sample sizes, which could affect its reliability in certain cases. Moreover, due to the lack of commercially available research models for the CF-TiZr and TF-Ti groups, the validation was limited to the CF-Ti and TF-TiZr groups. Nevertheless, this limitation can still provide valuable insights into the accuracy of model creation and enhance the informativeness of the stress results. Furthermore, whereas the static loading mode utilized in this study has been implemented in numerous established experimental models, the selection and refinement of loading modes may offer a more precise representation of clinical outcomes. Although this study was the first to examine the newly introduced implant-abutment connection (IAC) TF, it was solely compared to the already established implant-abutment connection of the same brand. As a result, the study's limitation lies in its focus on only one implant system and two IACs; therefore, the findings should not be extrapolated to other implant systems and IACs.

Conclusion
Changes in the implant alloy type had no significant impact on the maximum stress of the abutment, screw, or investment materials. However, it did affect the maximum stress of the implant itself. Variations in structural differences result in varying sensitivities of implant systems to changes in implant materials. Nevertheless, the TF groups exhibited sufficient stability and reliability even with such changes. This study provides a valuable modeling reference for clinicians when selecting an appropriate implant-abutment connection system. Furthermore, this study can assist dental implant researchers in optimizing the design of dental implants while also acknowledging the limitations of this FEA.

Anniwaer *et al. BMC Oral Health*   (2024) 24:901

Page 10 of 11

Declarations

Ethics approval and consent to participate
Not applicable.

Consent for publication
Not applicable.

Competing interests
The authors declare no competing interests.

References
1. Brånemark PI, Adell R, Albrektsson T, Lekholm U, Lundkvist S, Rockler B. Osseo-integrated titanium fixtures in the treatment of edentulousness. Biomaterials. 1983;4:25–8. https://doi.org/10.1016/0142-9612(83)90065-0.
2. I Z, Az SKAS. Assessing the effect of dental implants thread design on distribution of stress in impact loadings using three dimensional finite element method. J Dent Biomater. 2016;3:233–40.
3. Mosavar A, Ziaei A, Kadkhodaei M. The effect of implant thread design on stress distribution in anisotropic bone with different osseointegration conditions: a finite element analysis. Int J Oral Maxillofac Implants. 2015;30:1317–26. https://doi.org/10.11607/jomi.4091.
4. Ferraz CC, Anchieta RB, de Almeida EO, Freitas AC Jr, Ferraz FC, Machado LS, Rocha EP. Influence of microthreads and platform switching on stress distribution in bone using angled abutments. J Prosthodont Res. 2012;56:256–63. https://doi.org/10.1016/j.jpor.2012.02.002.
5. Brägger U. Etiology and origin of Hardware complications. In: Brägger U, editor. L. J. A. Heitz-Mayfield. ITI Treatment Guide Biological and Hardware complications in Implant Dentistry. Volume 8. Berlin: Quintessence Publishing Co; 2015. p. 114.
6. Lemos CAA, Verri FR, Noritomi PY, Kemmoku DT, Souza Batista VE, Cruz RS, de Luna Gomes JM, Pellizzer EP. Effect of bone quality and bone loss level around internal and external connection implants: a finite element analysis study. J Prosthet Dent. 2021;125:137e1. 137.e10.
7. Körtvélyessy G, Szabó ÁL, Pelsőczi-Kovács I, Tarjányi T, Tóth Z, Kárpáti K, Matusovits D, Hangyási BD, Baráth Z. Different conical angle connection of implant and abutment behavior: a static and dynamic load test and finite element analysis study. Mater (Basel). 2023;16:1988. https://doi.org/10.3390/ma16051988.
8. Yang F, Ruan Y, Liu Y, Chen J, Chen Y, Zhang W, Ding Y, Wang L. Abutment mechanical complications of a Morse taper connection implant system: a 1- to 9-year retrospective study. Clin Implant Dent Relat Res. 2022;24:683–95. https://doi.org/10.1111/cid.13115.
9. Al-Nawas B, Lambert F, Andersen SWM, Bornstein MM, Gahlert M, Jokstad A, Jung J, Kwon YD, Laleman I, Oteri G, Roehling S, Schiegnitz E, Takeda Y, Terheyden H. Group 3 ITI Consensus Report: materials and antiresorptive drug-associated outcomes in implant dentistry. Clin Oral Implants Res. 2023;34(Suppl 26):169–76.
10. Jiang J, Zhou C, Zhao Y, He F, Wang X. Development and properties of dental Ti-Zr binary alloys. J Mech Behav Biomed Mater. 2020;112:104048. https://doi.org/10.1016/j.jmbbm.2020.104048.
11. Sarraf M, Rezvani Ghomi E, Alipour S, Ramakrishna S, Liana Sukiman N. A state-of-the-art review of the fabrication and characteristics of titanium and its alloys for biomedical applications. Biodes Manuf. 2022;5:371–95. https://doi.org/10.1007/s42242-021-00170-3.
12. Sadowsky SJ. Has Zirconia made a material difference in implant prosthodontics? A review. Dent Mater. 2020;36:1–8. https://doi.org/10.1016/j.dental.2019.08.100.
13. Queiroz DA, Hagee N, Lee DJ, Zheng F. The behavior of a zirconia or metal abutment on the implant-abutment interface during cyclic loading. J Prosthet Dent. 2020;124:211–6. https://doi.org/10.1016/j.prosdent.2019.09.023.
14. Sailer I, Asgeirsson AG, Thoma DS, Fehmer V, Aspelund T, Özcan M, Pjetursson BE. Fracture strength of zirconia implant abutments on narrow diameter implants with internal and external implant abutment connections: a study on the titanium resin base concept. Clin Oral Implants Res. 2018;29:411–23. https://doi.org/10.1111/clr.13139.
15. Brandão de Holanda KA, Armini Caldas R, Amaral M, da Silva Concilio LR, Pino Vitti R. Biomechanical evaluation of anterior implants associated with titanium and zirconia abutments and monotype zirconia implants. J Prosthodont Res. 2021;65:73–7. https://doi.org/10.2186/jpr.JPOR_2019_527.
16. Kitagawa T, Tanimoto Y, Iida T, Murakami H. Effects of material and coefficient of friction on taper joint dental implants. J Prosthodont Res. 2020;64:359–67. https://doi.org/10.1016/j.jpor.2019.10.003.
17. Sharma A, Waddell JN, Li KC, Sharma A, Prior L, Duncan DJ. Is titanium-zirconium alloy a better alternative to pure titanium for oral implant? Composition, mechanical properties, and microstructure analysis. Saudi Dent J. 2021;33:546–53. https://doi.org/10.1016/j.sdentj.2020.08.009.
18. Cinel S, Celik E, Sagirkaya E, Sahin O. Experimental evaluation of stress distribution with narrow diameter implants: a finite element analysis. J Prosthet Dent. 2018;119:417–25. https://doi.org/10.1016/j.prosdent.2017.04.024.
19. Semlitsch M, Staub F, Weber H. Titanium-aluminium-niobium alloy, development for biocompatible, high strength surgical implants. Biomed Tech (Berl). 1985;30:334–9. https://doi.org/10.1515/bmte.1985.30.12.334.
20. Raju M, Ramadoss R, Vetrivel Sezhian M, Mithunkanna B. Finite element simulation of the tensile behavior of Ti-6Al-7Nb titanium alloy at elevated temperatures. Int J Interact Des M. 2023;17:1225–35. https://doi.org/10.1007/s12008-022-01103-9.
21. Dal Piva AMO, Tribst JPM, Borges ALS, Souza ROAE, Bottino MA. CAD-FEA modeling and analysis of different full crown monolithic restorations. Dent Mater. 2018;34:1342–50. https://doi.org/10.1016/j.dental.2018.06.024.
22. Silva LS, Verri FR, Lemos CAA, Martins CM, Pellizzer EP, de Souza Batista VE. Biomechanical effect of an occlusal device for patients with an implant-supported fixed dental prosthesis under parafunctional loading: a 3D finite element analysis. J Prosthet Dent. 2021;126:223. .e1-223.e8.
23. Silva NR, Calamia CS, Harsono M, Carvalho RM, Pegoraro LF, Fernandes CA, Vieira AC, Thompson VP. Bond angle effects on microtensile bonds: laboratory and FEA comparison. Dent Mater. 2006;22:314–24. https://doi.org/10.1016/j.dental.2005.05.006.
24. de Oliveira Silva TS, Mendes Alencar SM, da Silva Valente V, de Moura CDVS. Effect of internal hexagonal index on removal torque and tensile removal force of different Morse taper connection abutments. J Prosthet Dent. 2017;117:621–27. https://doi.org/10.1016/j.prosdent.2016.07.024.
25. Yilmaz B, Alsaery A, Altintas SH, Schimmel M. Comparison of strains for new generation CAD-CAM implant-supported crowns under loading. Clin Implant Dent Relat Res. 2020;22:397–402. https://doi.org/10.1111/cid.12894.
26. Pirmoradian M, Naeeni HA, Firouzbakht M, Toghraie D, Khabaz MK, Darabi R. Finite element analysis and experimental evaluation on stress distribution and sensitivity of dental implants to assess optimum length and thread pitch. Comput Methods Programs Biomed. 2020;187:105258.
27. Entezari A, Zhang Z, Sue A, Sun G, Huo X, Chang CC, Zhou S, Swain MV, Li Q. Nondestructive characterization of bone tissue scaffolds for clinical scenarios. J Mech Behav Biomed Mater. 2019;89:150–61. https://doi.org/10.1016/j.jmbbm.2018.08.034.
28. de Pereira HC, de Oliveira Limirio AK, Cavalcanti do Egito Vasconcelos JPJ, Pellizzer B, Dantas de Moraes EP. Mechanical behavior of titanium and

zirconia abutments at the implant-abutment interface: a systematic review. J Prosthet Dent. 2022. https://doi.org/10.1016/j.prosdent.2022.01.006. S0022-391300050-6.

29. Queiroz DA, Hagee N, Lee DJ, Zheng F. The behavior of a zirconia or metal abutment on the implant-abutment interface during cyclic loading. J Prosthet Dent. 2020;124:211–16. https://doi.org/10.1016/j.prosdent.2019.09.023.

30. Datte CE, Tribst JP, Dal Piva AO, Nishioka RS, Bottino MA, Evangelhista AM, Monteiro FMM, Borges AL. Influence of different restorative materials on the stress distribution in dental implants. J Clin Exp Dent. 2018;10:e439–44. https://doi.org/10.4317/jced.54554.

31. Matta RE, Berger L, Loehlein M, Leven L, Taxis J, Wichmann M, Motel C. Stress distribution within the Peri-implant bone for different Implant materials obtained by digital image correlation. Mater (Basel). 2024;17:2161. https://doi.org/10.3390/ma17092161.

32. Araki H, Nakano T, Ono S, Yatani H. Three-dimensional finite element analysis of extra short implants focusing on implant designs and materials. Int J Implant Dent. 2020;6:5. https://doi.org/10.1186/s40729-019-0202-6.

33. Blum K, Wiest W, Fella C, Balles A, Dittmann J, Rack A, Maier D, Thomann R, Spies BC, Kohal RJ, Zabler S, Nelson K. Fatigue induced changes in conical implant-abutment connections. Dent Mater. 2015;31:1415–26. https://doi.org/10.1016/j.dental.2015.09.004.

34. Yu X, Han Y, Wang J. Is an internal tapered connection more efficient than an internal nontapered connection? A systematic review and meta-analysis. J Prosthet Dent. 2020;124:431–38. https://doi.org/10.1016/j.prosdent.2019.07.018.

35. Rodrigues VVM, Faé DS, Rosa CDDRD, Bento VAA, Lacerda MFLS, Pellizzer EP, Lemos CAA. Is the clinical performance of internal conical connection better than internal non-conical connection for implant-supported restorations? A systematic review with meta-analysis of randomized controlled trials. J Prosthodont. 2023;32:382–91. https://doi.org/10.1111/jopr.13655.

36. Kwan JC, Kwan N. The effects of a vertical compressive cyclic load on abutment screws and the stability of the prosthesis in nonengaging and partially engaging abutments in a screw-retained splinted fixed dental prosthesis. Int J Oral Maxillofac Implants. 2022;37:571–78. https://doi.org/10.11607/jomi.9542.

37. Kofron MD, Carstens M, Fu C, Wen HB. In vitro assessment of connection strength and stability of internal implant-abutment connections. Clin Biomech (Bristol Avon). 2019;65:92–9. https://doi.org/10.1016/j.clinbiomech.2019.03.007.

38. Khongkhunthian P, Khongkhunthian S, Weerawatprachya W, Pongpat K, Aunmeungtong W. Comparative study of torque resistance and microgaps between a combined Octatorx-cone connection and an internal hexagon implant-abutment connection. J Prosthet Dent. 2015;113:420–4. https://doi.org/10.1016/j.prosdent.2014.12.006.

39. Çakmak G, Güven ME, Donmez MB, Kahveci Ç, Schimmel M, Abou-Ayash S, Yilmaz B. Effect of internal connection type and screw channel angle on the screw stability of anterior implant-supported zirconia crowns. Clin Oral Implants Res. 2023;34:1248–56. https://doi.org/10.1111/clr.14165.

40. Vargas-Isaza C, Posada-Correa J, Briñez-de León J. Analysis of the stress field in photoelasticity ssed to evaluate the residual stresses of a plastic injection-molded part. Polym (Basel). 2023;15:3377. https://doi.org/10.3390/polym15163377.

41. Baghiana G, Manju V, Hariprasad MP, Menon HG, Dutta S, Gopal VK, Deepthy SS. Comparison of attachment types in Maxillary Implant-assisted obturators using digital image correlation analysis. J Contemp Dent Pract. 2022;23:695–702.

42. Qiao Y, Guan XB, Zhang ZX. Experimental study on crack propagation pattern and fracture process zone evolution based on far-field displacement by using DIC. Sci Rep. 2023;13:19523. https://doi.org/10.1038/s41598-023-44458-z.

43. Freitas MIM, Gomes RS, Ruggiero MM, Bergamo ETP, Bonfante EA, Marcello-Machado RM, Del Bel Cury AA. Probability of survival and stress distribution of narrow diameter implants with different implant-abutment taper angles. J Biomed Mater Res B Appl Biomater. 2022;110:638–45. https://doi.org/10.1002/jbm.b.34942.

44. Chen J, Wang L, Yang L, Zhang X, Huang B, Li J. The prosthetic screw loosening of two-implant supported screw-retained fixed dental prostheses in the posterior region: a retrospective evaluation and finite element analysis. J Biomech. 2021;122:110423. https://doi.org/10.1016/j.jbiomech.2021.110423.

Publisher's Note